Numerical assessment of a cognitive chamber: TM^z case

Christophe Craeye*, Sidina Wane†, Khaldoun Alkhalifeh†, Denis Tihon*
ICTEAM Institute, UCLouvain, Louvain-la-Neuve, Belgium
†eV-Technologies, Caen, France
corresponding author: christophe.craeye@uclouvain.be

***Abstract*—A numerical analysis based on the Method of Moments is conducted to study the feasibility of absorbing chambers made of arrays of metallic elements, named here as *cognitive chambers*. The array is covering the inner surface of a perfectly conducting cylindrical shield. The analysis is so far limited to the TM^z case. Very low perturbation of the field from a device under test, represented by a collection of axial dipoles is observed. The non-disturbance of the incident fields correlates well with a criterion based on the active impedance. A significant dependence of the optimal load impedance versus azimuthal and axial modes has been observed.**

***Index Terms*—antenna arrays, mutual coupling, cognitive chamber, absorption.**

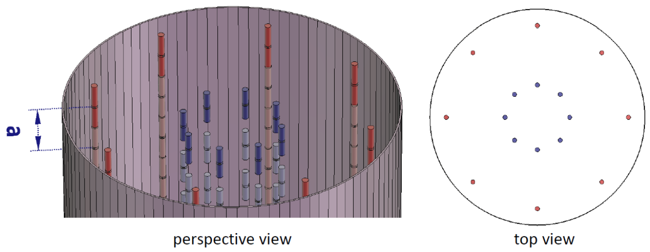

Fig. 1. Cognitive chamber structure. Left: perspective view. Right: cross section. Blue: transmitting DUT. Red: receiving dipoles, part of the chamber.

I. Introduction

With the high-rate production of devices devoted to communications and radar, an increased need appeared for automatic industrial verification. Ideally, the radiated fields should be observed in all directions, in the near-to-intermediate field, without disturbing the fields near the device under test (DUT). To this end, one may use dense arrays of antennas surrounding the DUT. Such arrays may also allow source inversion as well as the measurement of correlation between fields [1]–[3] in arbitrary directions. Although the envisaged antennas are metallic and are covering the surface of a shielded room, without any absorbing material, the goal is to achieve a nearly total absorption and virtually zero-scattering of the fields radiated by the DUT. Given the goals announced above, such arrays will be named *cognitive chambers*.

Regarding the observation of electromagnetic fields at RF or microwave frequencies, hemispherical and cylindrical configurations are very common in medical applications, given their ability to fully scan the object. Craddock et al. used a hemispherical 60-element antenna array devoted to breast cancer detection. It operates as a multistatic radar system in the 4–8 GHz frequency range [4]. Fear et al. used cylindrical imaging systems to localize breast tumors in three dimensions [5]. The MVG vertical arch system, generally used in vehicle measurement applications, has been transposed to a horizontal-axis arch of sensors, which enables 3D multi-static short-range radar imaging [6]. However, those systems all involve either absorbing material or matching liquid. The *cognitive chamber* studied here only comprises a metallic shield and properly loaded metallic antennas. One might expect important challenges in terms of standing waves in the shielded space, but one should remember that, for instance, planar arrays are known to be able to absorb *all the incident power* in a broad range of incidence angles and frequencies, if matched in the active impedance sense [7], [8], [9].

In order to benefit from symmetry and hence to envisage the use of elements that are all identical, a cylindrical structure [10] is analyzed here. It is made long in the axial direction, such that an infinite-array approximation would be representative[1]. Henceforth, the structure will be named as a *Cylindrical Cognitive Chambers* (see Fig. 1). In this paper, the analysis is limited to transmitting and receiving dipoles that are parallel to the cylinder axis, which corresponds to the TM^z case.

The remainder of this paper is organized as follows. In Section 2, the analysis technique is briefly described and in Section 3 the optimal loading of the receiving antennas is analyzed based on a criterion related to the active impedance of the transmitting antennas serving as DUT (device under test). Brief conclusions and perspectives are drawn in Section 4.

II. Method-of-Moments analysis

The structure to be analyzed is sketched in Figure 1. It consists of a conducting cylinder and N_a dipoles (red). The dipoles are equally distributed, close to the cylinder edge (typically at a quarter of the wavelength λ). The N_a inner dipoles (blue in Figure 1) stand for the device under test (DUT); they transmit either jointly or in isolation. The structure is periodic along the azimuth ϕ, with N_a antennas over 2π radian and it is also periodic along the axis of the chamber

[1]Mitigation methods able to ensure absorption at the ends of the cylinder will be studied later.

(Z axis), with period a. It is known that isolated sources can be represented as a spectrum of sources spread over planes, spheres or cylinders [11]. The latter case is considered here. That is why we allow a certain phase shift between consecutive transmitting elements along the Z axis, as well as all integer multiples of $2\pi/N_a$ phase shifts along the azimuth. Hence, the Green's function used here corresponds to that of infinite arrays aligned along $\hat{z}$, with an inter-element phase shift equal to $k_z^0\, a$. In this configuration, only the z component of current sources and electric fields needs to be considered. This hence requires the use of the following Green's function [12]:

$$G^{zz} = \frac{-j\, k_\circ\, \eta}{4\, j\, a} \sum_p H_0^{(2)}(k_\rho^p\, \rho)\; e^{j\, k_z^p\, z}\; \left(k_\rho^p / k_\circ\right)^2 \qquad (1)$$

where $k_\circ$ is the free-space wavenumber, η is the free-space impedance, and $H_0^{(2)}(.)$ is the Hankel function of order 0 and type 2. Each term in the summation corresponds to the contribution of a different Floquet wavenumber k_z^p

$$k_z^p = k_z^0 + p\, \frac{2\pi}{a} \quad \text{with} \quad (k_\rho^p)^2 + (k_z^p)^2 = k_\circ^2 \qquad (2)$$

Variable ρ corresponds to the distance between transmitting current and observed field positions, both projected in a plane perpendicular to z.

A wire radius of $\lambda/200$ is considered, which allows the use of Pocklington's thin-wire approximation [14]. The shield is made of wires with same radius as that of the transmitting and receiving antennas, with a high density, with spacings of the order of a $\lambda/20$. In a method-of-moments framework, the use of the periodic Green's function allows a spectral-domain evaluation of the interactions between basis and testing functions:

$$Z(i,j) = \sum_p G^{zz}(k_z^p, \rho_{ij})\; \tilde{F}_i(k_z^p)\; \tilde{F}_j(-k_z^p) \qquad (3)$$

where $\tilde{F}_i(k_z)$ is the Fourier transform of a given basis or testing function. In this paper, the basis and testing functions correspond to symmetrical triangles of width L along the z coordinate, such that $\tilde{F}(k_z) = L/2\,(\sin x/x)^2$ with $x = k_z\, L/4$.

It is important to note that the spectral series (1) does not converge well for small values of ρ. This is why a space-domain approach is adopted when ρ is smaller than a tenth of the wavelength [13]. This goes in several steps. First, the Green's function is tabulated versus z and ρ over the unit cell. A space domain summation, vastly accelerated with Levin's series extrapolator [16] is used. The contribution of the reference dipole (self-term) is excluded from the series, and the double convolution involved in the evaluation of the $Z(i,j)$ elements is carried out in space domain. The contribution of the self-term is added afterwards, based on a classical approach including the analytical extraction of the $1/R$ singularity. Details about the mathematical formulation of this near-field case will be provided in a later publication.

The analysed structure being a discrete body of revolution, it allows a matrix-filling time, but also a solution time, that are simply proportional to the number N_a of sectors (here the number of receving antennas along the periphery of the structure) [15]. In the following, excitations of type $\exp(j\, m\, \phi)$ with different indices m will be named *azimuthal* modes. Likewise, different phase shifts along z, obtained as $\psi_z = k_{z,\circ}\, a$ will be named *axial modes*[2]. Translational symmetry among the basis functions defined on the shield has also been exploited to vastly accelerate the filling of the MoM impedance matrix.

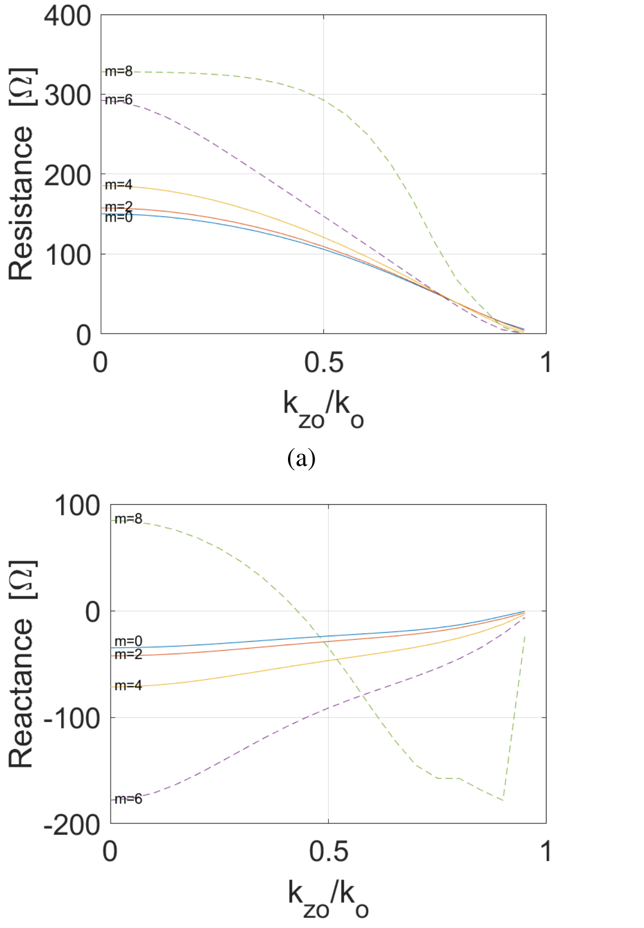

(a)

(b)

Fig. 2. Optimal resistances (a) and reactances (b) for orders $m = 0$, 2, 4, 6 and 8 azimuthal mode versus axial wavenumber.

III. Validation and absorbing array performance

Numerical consistency checks are necessary to assess the accuracy of the numerical implementation. First, one verifies that the field outside the cylinder is close to zero, which is not a priori imposed by the MoM approach. The fields outside have been observed to be typically 32 dB below[3] those inside. Second, we checked that the power fed by the transmitting antennas is absorbed by the loads of the receiving antennas,

[2] Azimuthal and axial modes come in discrete and continuous spectra, respectively

[3] A higher density for the wires making up the shield may bring that value further down

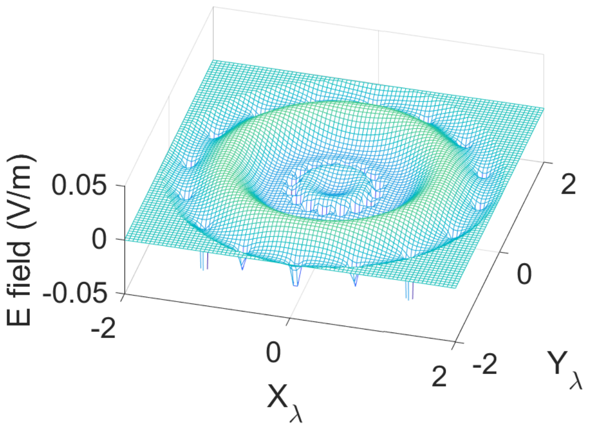

Fig. 3. Total field in presence of cognitive chamber. All transmitters excited, $m = 0$, $k_z = 0$.

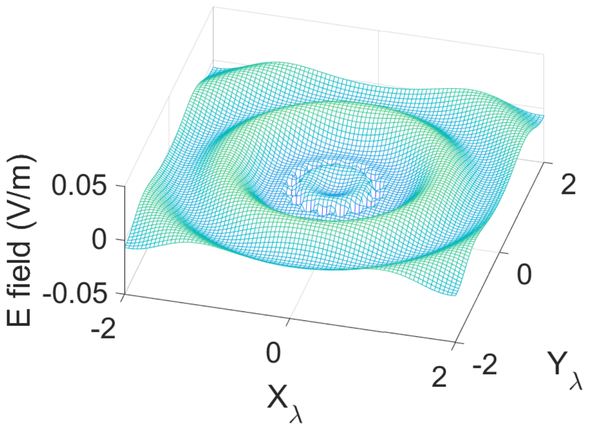

Fig. 4. Total field in absence of cognitive chamber. All transmitters excited, $m = 0$, $k_z = 0$.

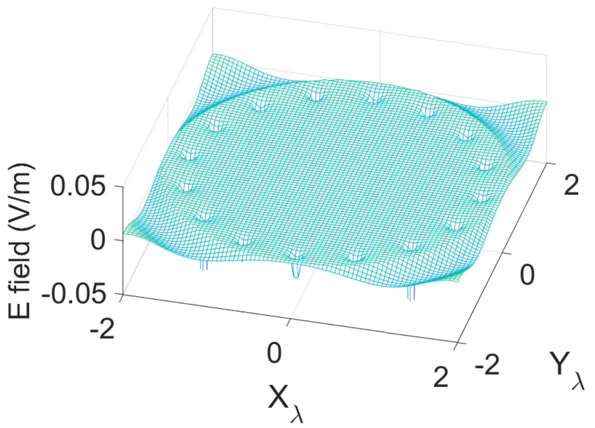

Fig. 5. Difference between fields in presence of cognitive chamber and reference fields All transmitters excited, $m = 0$, $k_z = 0$.

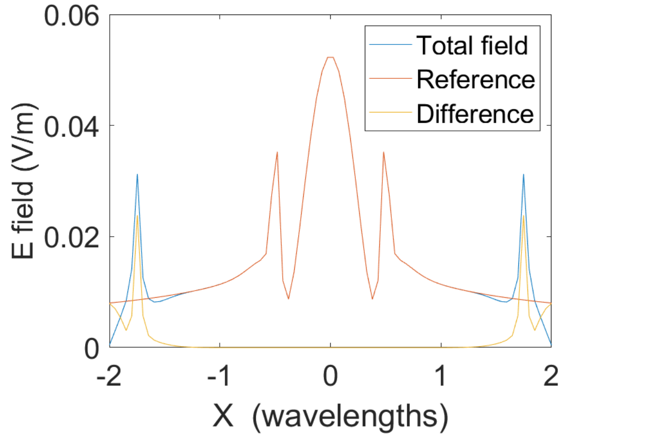

Fig. 6. Fields in presence of cognitive chamber (”total”) with source offset of 0.5 wavelength, as well as reference (no chamber) and difference. All transmitters excited, $m = 0$, $k_z = 0$.

which is typically satisfied within 0.1 percent, despite the fact that the MoM does not explicitly enforce energy conservation. It is important to notice here that this must always be satisfied, even when the chamber is strongly scattering. However, a good design is supposed not to disturb the DUT, which is verified by minimizing the change of its active impedance (see below). As a third check, we also verified that, when the loads terminating the chamber's antennas are set to zero or virtually to infinity, the transmitting antennas do not transmit any real power, which translates into the fact that their active impedance is nearly imaginary. We observed that in those cases the imaginary part of the DUT's active impedance is about four orders of magnitude larger than its real part.

A minimum-scattering design supposes a sufficiently dense array of receiving elements, with appropriate dipole lengths and distance from the shield. This also supposes an appropriately optimized load. Examples are shown in this section. They refer to a chamber with a 4 λ diameter and $N_a = 16$ elements along its periphery, with a length of 0.488 λ and a $\lambda/4$ distance from the shield, while the transmitting antennas, representing the DUT, are placed either at 0.25 λ or 0.5 λ from the center and have a length of 0.34 λ.

The optimal impedance is obtained by ensuring that the chamber does not scatter at the level of the transmitting antennas, i.e. such that the active impedance of the antennas serving here as a DUT does not change when the chamber is added. We observe that the optimal loads have a significant dependence on the azimuthal and axial mode indices. As mentioned in Section 2, the radiation from a non-centered source can be written as a double spectrum of waves along those indices; it is hence expected that a compromise will need to be found for the loading of the antennas. Figure 2 shows the optimal impedance obtained versus the k_z wavenumber and versus the axial mode index m for a DUT located at 0.25 λ from the center. For clarity, only even modes up to $N_a/2$ are

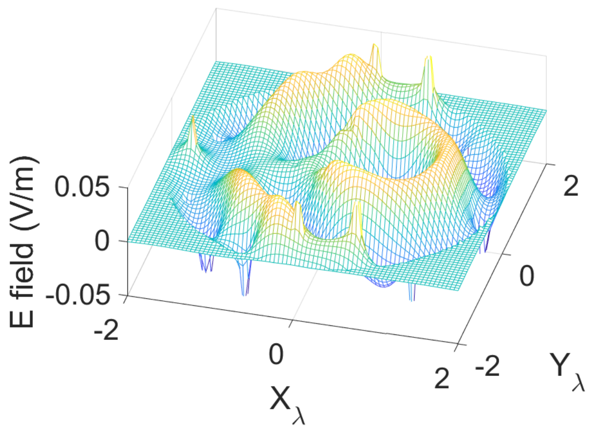

Fig. 7. Total field in presence of cognitive chamber for one element excited, at 0.5 wavelength from center; $k_z = 0$.

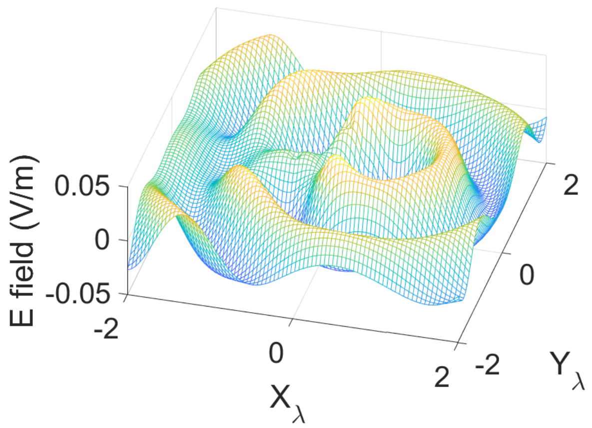

Fig. 8. Reference field in absence of cognitive chamber for one element excited, at 0.5 wavelength from center; $k_z = 0$.

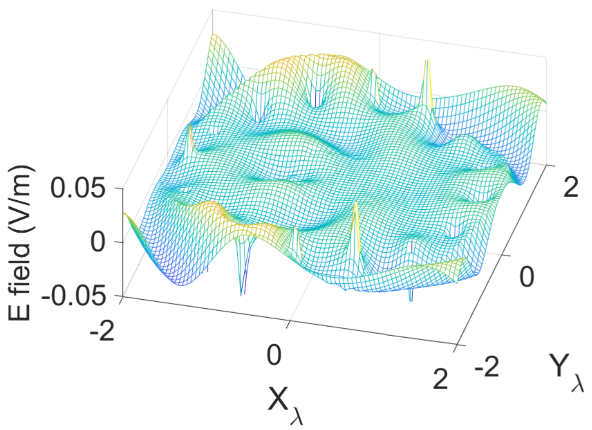

Fig. 9. Difference between fields in presence of cognitive chamber and reference fields, for one element excited, at 0.5 wavelength from center; $k_z = 0$.

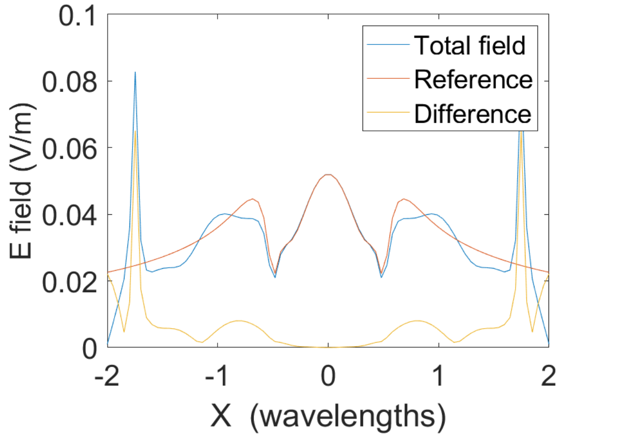

Fig. 10. Fields in presence of cognitive chamber (”total”) with source offset of 0.5 wavelength, as well as reference (no chamber) and difference; $k_z = 0$.

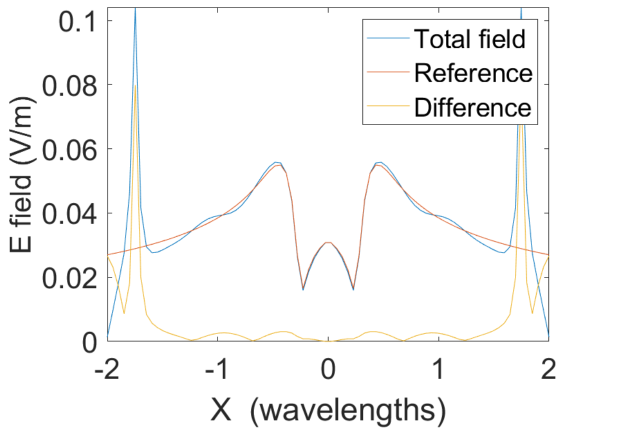

Fig. 11. Fields in presence of cognitive chamber (”total”) with source offset of 0.25 wavelengths, as well as reference (no chamber) and difference; $k_z = 0$.

shown[4]). High-order azimuthal modes are denoted with dashed lines, since they actually produce waves that are evanescent versus radius, which do not truly reach the receiving antennas. Given the significant dependence of the optimal load on modal index, solutions with adaptive loading might also be envisaged [17].

For $m = 0$ and $k_z = 0$, the optimal impedance is here $150.4 - j\,34.9\,\Omega$. Figure 3 shows the total field obtained within the chamber, to be compared with the fields without the chamber (i.e. DUT only), in Figure 4. The difference between the fields is shown in Figure 5. It is observed that, within the chamber, in a disk excluding the absorbing antennas, the scattering by the chamber is very well suppressed. A cut of the fields passing through the center is shown in Figure 6. The sharp peaks correspond to the positions of transmitting (DUT) and receiving (near shield) antennas.

As explained above, the optimal impedance depends on the

[4]Odd modes do not have a specifically different behavior; modes with index $m > N_a/2$ behave identically to the mode $N_a - m$.

modal index. Let us now consider this dependence along index m for $k_z = 0$. To represent a DUT that is not centered or a DUT of a certain size, several m indices will be necessary. For instance, excitation at element 0 only can be represented by the superposition of all modes with all elements excited. This stems from the fact that the Fourier transform of a discrete delta function is a constant. A priori, only one specific loading of the antennas is possible. Hence such a simulation is carried out with the optimal load referred to above, obtained for $m = 0$. Figures 7 to 9 show the total, reference and difference fields obtained in that case, for a source shifted by $\lambda/2$ from the center and $k_z = 0$. A larger perturbation of the fields is observed[5]. This is due to the fact that the used loading, related to the $m = 0$ mode, is not truly appropriate for higher-order modes. A cut of the fields passing through the center is shown in Figure 10. The same cut is represented in Figure 11, for a smaller shift of the source, by 0.25 wavelengths; it can be seen that in the latter case the obtained scattering is much smaller.

IV. Conclusion

A MoM software has been developed to analyze cylindrical absorbing arrays, or *cognitive chambers*, so far limited to the TM^z case. Several improvements made it efficient and a number of sanity checks, including energy conservation, allowed its validation. We showed that, for a small DUT, the elements distributed along the inner surface of the cylinder allowed a nearly total absorption of power, without strong perturbation of the fields radiated by the DUT, which radiate almost as if it were located in free space. At the same time, it is possible to observe and cross-correlate the fields at the level of each receiving dipole. Further improvements of the analysis will obviously include the introduction of a TE^z component, as well as an analytical determination of the optimal loads and a strategy to deal with or to find a compromise for the dependence of those loads to the azimuthal or axial mode index. Such improvements are expected to enable the characterization of larger DUT's. The bandwidth of operation of cognitive chambers remains to be studied and eventually optimized by making use of other types of antennas along the chamber's wall. Such radiators may correspond to tapered-slot antennas, as realized in [18] for inward-looking circular arrays.

References

[1] D. Tihon, S. Withington, C.N. Thomas, C. Craeye, "Characterization of power absorption response of periodic three-dimensional structures to partially coherent fields," *JOSA A*, vol. 33, pp. 2459-2469, Dec. 2016.

[2] G. Gradoni, J. Russer, M.H. Baharuddin, M. Haider, P. Russer, C. Smartt and D. W. Thomas, "Stochastic electromagnetic field propagation—measurement and modelling," *Phil. Trans. Royal Soc. A*, vol. 376, no. 2134, pp. 1-20, 2018.

[3] S. Wane, C-S. Park, C. Craeye, "Device and method for simultaneous detection of incident electric and magnetic fields, as well as energy crossing a given surface," WO2023166228, March 6, 2023.

[4] D. Byrne, M. Sarafianou and I. J. Craddock, "Compound Radar Approach for Breast Imaging," *IEEE Trans. Biomedical Eng.*, vol. 64, no. 1, pp. 40-51, Jan. 2017.

[5]High fields near the edges of the difference figure should not be considered, since they correspond to the opposite of incident fields outside the cylinder

[5] E. C. Fear, X. Li, S. C. Hagness and M. A. Stuchly, "Confocal microwave imaging for breast cancer detection: localization of tumors in three dimensions," *IEEE Trans. Biomedical Eng.*, vol. 49, no. 8, pp. 812-822, Aug. 2002.

[6] A. Fasoula, S. Anwar, Y. Toutain and L. Duchesne, "Microwave vision: From RF safety to medical imaging," *11th Eur. Conf. Antennas Propag. (EUCAP),* Paris, pp. 2746-2750, March 2017.

[7] P. Hannan, "The element-gain paradox for a phased-array antenna," *IEEE Trans. Antennas Propag.,* Vol. 12, no. 4, 423–433, 1964.

[8] H. Holter, T.-H. Chio and D. H. Schaubert, "Experimental results of 144-element dual-polarized endfire tapered-slot phased arrays," *IEEE Trans. Antennas Propag.*, vol. 48, no. 11, pp. 1707-1718, Nov. 2000.

[9] C. Craeye and M. Arts, "On the receiving cross section of an antenna in infinite linear and planar arrays," *Radio Science,* Vol. 39, 25 pp., Apr. 2004.

[10] S. Wane, Kh. Alkhalifeh, C. Craeye, "Device and method for imaging stochastic fields using correlation functions in multi-level 3D conformal arrays," EP22305634.2, April 2022.

[11] Z. Šipuš, P.S. Kildal, R. Leijon, M. Johansson, "An algorithm for calculating Green's functions of planar, circular cylindrical and spherical multilayer substrates," *Appl. Comput. Electromagn. Soc. Journ.* vol. 13, no. 3, pp. 243-254, 1998.

[12] R.J. Mailloux, "Phased array theory and technology," *Proc. IEEE,* vol. 70, no. 3, pp. 246–291.

[13] C. Craeye, A. G. Tijhuis and D. H. Schaubert, "An efficient MoM formulation for finite-by-infinite arrays of two-dimensional antennas arranged in a three-dimensional structure," *IEEE Trans. Antennas Propag.*, vol. 52, no. 1, pp. 271-282, Jan. 2004.

[14] R.F. Harrington "Matrix methods for field problems," *Proceedings of the IEEE,* vol. 55, pp. 136-149, 1967.

[15] R. Vescovo, "Inversion of block-circulant matrices and circular array approach," *IEEE Trans. Antennas Propag.*, vol. 45, no. 10, pp. 1565-1567, Oct. 1997.

[16] S. Singh and R. Singh, "On the use of Levin's T-transform in accelerating the summation of series representing the free-space periodic Green's functions," *IEEE Trans. Microwave Theory Techn.,* vol. 41, pp. 884–886, May 1993.

[17] S. Wane, V. Huard, M. Rack, L. Nyssens, B. Kieniewicz, D. Bajon, J.-P. Raskin, "Broadband smart mmWave front-end-modules in advanced FD-SOI with adaptive-biasing and tuning of distributed antenna-arrays," 2020 IEEE Texas Symp. Wireless Microw. Circ. Syst. (WMCS), Waco, TX, USA, pp. 1-5, May 2020.

[18] Kh. Alkhalifeh, R. Sarkis, C. Craeye, "Wheel-of-time array devoted to near-field imaging applications," *2013 Int. Conf. Electromagn. Adv. Appl. (ICEAA)* pp. 1164-1167, Torino, Sep. 2013.